

Article

# Experimental Study on Temperature Change and Crack Expansion of High Temperature Granite under Different Cooling Shock Treatments

Yan-Jun Shen <sup>1,\*</sup> , Xin Hou <sup>2</sup>, Jiang-Qiang Yuan <sup>2</sup> and Chun-Hu Zhao <sup>3</sup>

<sup>1</sup> Geological Research Institute for Coal Green Mining, Xi'an University of Science and Technology, Xi'an 710054, China

<sup>2</sup> School of Architecture and Civil Engineering, Xi'an University of Science and Technology, Xi'an 710054, China; 17204209083@stu.xust.edu.cn (X.H.); 17605203751@163.com (J.-Q.Y.)

<sup>3</sup> Xi'an Research Institute Co. Ltd., China Coal Technology and Engineering Group Corp., Xi'an 710077, China; zhaochunhu@cctegxian.com

\* Correspondence: shenyj@xust.edu.cn; Tel.: +86-153-5356-8720

Received: 2 May 2019; Accepted: 29 May 2019; Published: 31 May 2019



**Abstract:** It is valuable to observe the influence of different cooling methods on the exploitation of geothermal energy and breaking hard rocks in deep geo-engineering. In this work, the effects of different cooling shock treatments on high temperature granite are discussed. First, perforated 100-mm-side cubic biotite adamellite samples were heated to four targeted temperatures (150 °C, 350 °C, 550 °C, and 750 °C). Then, anti-freeze solutions were compounded to produce the different cooling shock effects (20 °C, 0 °C, and −30 °C) by adjusting the calcium chloride solution concentration, and these anti-freeze solutions were injected rapidly into the holes to reflect the rapid cooling shock of high-temperature granite. Finally, the temperature variations and crack expansions of high-temperature granite under different cooling shock treatments were analyzed and the cooling shock cracking mechanism is discussed briefly. The main results can be summarized as: (1) The high temperature granite exposed to the cooling shock exhibited a "rapid cooling + rapid heating" change during the first 5 min. Due to the cooling shock, the total temperature was significantly lower than the natural cooling until 120 min later. (2) Below 350 °C, the macrocracking effect was not significant, and the sample reflected a certain range of uniform microcracks around the injection hole, while the macrocracks tended to be obvious above 550 °C. Moreover, as the refrigerant temperature decreased, the local distribution characteristics of the macrocracking became more obvious. (3) Based on the analysis of the dynamic heat balance, the undulation and width of the cracks around the heat balance zone were stable, but the numbers and widths of cracks near the hole wall and the side of the sample were visibly increased. This study extends our understanding of the influence of cooling shock on granite cracking.

**Keywords:** high temperature granite; cooling shock; temperature change; crack expansion; dynamic heat balance

## 1. Introduction

Currently, the majority of human energy demands depend on the supply of fossil fuels. However, the use of carbon-based fuels for power generation affects the atmosphere and global climate [1,2]. In addition, as a nonrenewable resource, fossil fuels will eventually face the dilemma of resource exhaustion. There is increasing enthusiasm for finding new renewable energy sources to replace fossil fuels, thereby reducing dependence on fossil fuels and reducing or eliminating greenhouse gas emissions. Renewable energy sources (i.e., wind energy, solar energy, tidal energy, geothermal

energy) exhibit advantages such as high geothermal energy, stable and long-lasting energy, and low power generation costs. The proportion of geothermal energy in clean energy is increasing yearly [3,4], and geothermal energy, as a new clean energy, has become a focus of future development. Generally, geothermal energy was developed for heating, heat preservation, heat generation, and power generation [5]. Among the types of geothermal energy, the dry hot rock enhanced geothermal system (EGS) is widely used in power plant construction to extract thermal energy from the natural crust for power generation. However, the complex geological condition of the earth's crust, such as high temperature and strong geo-stress [6], causes a significant challenge to exploit the deep resources. For example, for EGS exploitation, a stable geothermal reservoir needs to be built in a high temperature rock mass area in order to obtain a good heat exchange. However, the current method is generally hydraulic fracturing under room temperature conditions (above zero), which cannot provide an efficient cracking effect and the good ability of heat exchange. Therefore, how to effectively improve the cracking effect and accelerate the water penetration rate among cracks in high temperature rock environments has become an important issue in the field of geothermal exploitation.

It is necessary to acquire the mechanical properties of high temperature hot dry rocks. Previous studies on high temperature rock have conducted numerous tests and obtained some valuable research findings. Yang et al. [7] have even conducted uniaxial compression tests of granite samples at different high temperature treatments (200, 300, 400, 500, 600, 700, and 800 °C), and obtained mechanical failure characteristics after high temperature treatments. Yin et al. [8] has also performed static mechanical tests, heating granite samples at different high temperatures (25, 200, 400, 600, and 800 °C). They found that the failure mode of granite was mainly caused by tensile failure when the temperature was lower than 100 °C. However, beyond 100 °C, the failure features were splitting and shearing damage. Guo et al. [9] carried out a series of triaxial tests to reflect the influence of temperature changes (from 30 °C to 150 °C) at different confining pressures on the mechanical properties of granite samples, and the results revealed that with the increases in temperature and confining pressure, the cracks expanded from vertical tilt to a single fracture surface, and the mechanical properties were continuously weakened. Related tests have also shown that, in the case of confining pressure, the difference in temperature also causes a greater impact on the rock and its mechanical properties often decrease with increasing temperature [10–12]. A series of tests have verified that thermal stress due to temperature differences between the interior and exterior of a granite body can cause an obvious cracking phenomenon [13–15]. Of course, the macroscopic cracks can cause a significant decrease in the mechanical properties of rocks. According to the results of Hosseini's experiments, as the number of thermal cycles increases, the longitudinal wave velocity and tensile strength decrease, and this causes the porosity to increase [16].

However, the thermo-damage seems to cease with additional heating cycles. Some studies have reported that the thermo-damage may reach a steady state after three repetitions of thermal cycling [17–19]. Therefore, in order to improve the breaking effects of the surrounding rocks for exploitation of the EGS, some new approaches have been carried out in recent decades. Among them, the cooling shock method, which can have a huge effect on temperature gradient, is regarded as a good attempt to produce better cracking. In particular, the method of rapid cooling on high temperature rocks can lead to a significant decrease in mechanical properties and cause considerable cracking after cold quenching, which is much greater than treatments without cold quenching according to previous reports [20–23]. Meanwhile, rapid cooling also has a great influence on the microstructure of rocks and causes their porosity and permeability to increase [24,25]. To date, previous experimental studies on this issue usually chose liquid water under a room temperature condition as a quenching material. However, a question that should be considered is whether a quenching liquid at lower temperatures will cause more significant damage to the rock. As a matter of fact, the use of liquid nitrogen, a very low temperature refrigerant with a limit of  $-196$  °C, can indeed cause a strong cold impact on high-temperature rocks and result in the mechanical properties decreasing with the amount of surface cracks. However, the damage resulting from such an extremely low temperature refrigerant

seems to not be very strong and cannot cause the integrated rock to completely break [26–28]. Moreover, the cost is relatively expensive. Therefore, it is not the most suitable method to use liquid nitrogen for the exploitation of the EGS.

In total, most previous studies on the topic of EGS exploitation have focused on the profile changes, and the physical and mechanical properties of granite samples exposed to high temperatures. Although a few studies concerning the cracking effects of cooling shock on high-temperature rocks have been conducted, the studies seem not to carry out a systematic experiment on the cracking caused by the refrigerant at different temperature gradients, especially for refrigerants at temperatures below 0 °C. Thus, this study focused on this issue of the impact that cooling shock at different temperature gradients has on high temperature granite samples and observed temperature changes and crack expansion during these tests. By dividing the refrigerants and granites into different temperature gradients, on the one hand, we studied the temperature change of granite due to the cooling shock of different temperature gradients, and on the other hand, we analyzed and summarized the cracking conditions and crack morphology of granite due to cooling shock. Under the cold impact of different temperature gradients, we studied in detail the temperature changes and cracking effects of granite at different temperatures. The results obtained in this experimental study provide a reference and significant guidance for the establishment of geothermal resource thermal storage layers and the simulation of the exploitation of deep oil and gas fields.

## 2. Materials and Methods

### 2.1. Rock Sample Preparation

According to the lithological characteristics of dry hot rocks of geothermal resources in China, granite is the most widely distributed rock type [29]. Therefore, in this study, granite samples are chosen as the test objectives to understand the physical and mechanical behaviors of dry hot rocks. The granite samples used in this experiment are from the Ganzi Prefecture of Sichuan Province, China (Figure 1), which is one of the richest geothermal resource areas. The granite is biotite adamellite. The mineral composition is mainly quartz, feldspar and biotite, with complex structure, different grain size, and dense texture. The granite samples were delivered to processing plants with stone cutters, and the rock samples were processed into cubes of 100 mm side lengths. This test used a rock drilling machine to drill holes into the center of the cube, with a drilling depth of 80 mm and a diameter of 30 mm, and then the surface of the sample was leveled and polished by a grinder. Finally, the 16 drilled cubes of granite rock samples were prepared for heating and quenching, and divided into four groups of rock samples. One group of granites was not subjected to the cooling shock treatment, and after heating these granites to the set temperature, they were allowed to cool to room temperature as a comparison group.

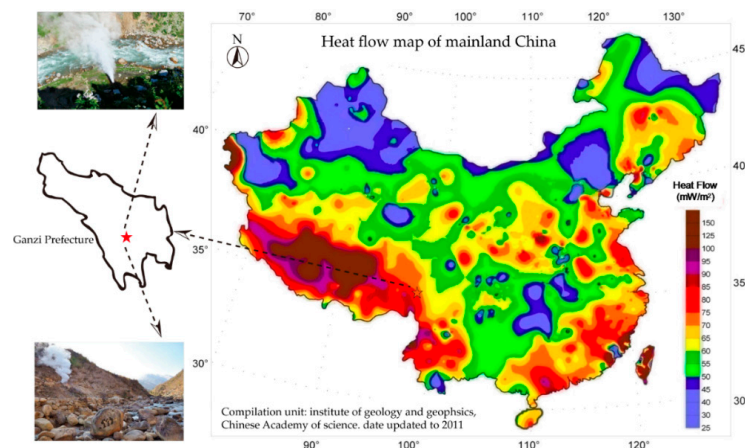


**Figure 1.** Location of the monzonitic quarry near the Ganzi geothermal well.

## 2.2. Refrigerant Preparation

To ensure the injectability of the refrigerant material, water, saturated sodium chloride and liquid nitrogen is generally used as the antifreeze solutions, and the test and various refrigerants used in this experiment are comprehensively considered. For the comparison of properties (corrosion, volatility, hot melt), a calcium chloride solution (Physical stability, freezing point  $-55\text{ }^{\circ}\text{C}$ ) was used as the experimental refrigerant. Using small particles of anhydrous calcium chloride (Brand name: Huakang, Zhengzhou, Henan Province, China), the calcium chloride solution was configured according to different freezing points of calcium chloride, and then the calcium chloride solution was adjusted to specific temperatures. The boxes were lowered to the preset temperature gradient and cooled for at least 24 hours in the temperature chamber to ensure that the calcium chloride solution reached the set temperature for a total of 3 gradients:  $-30\text{ }^{\circ}\text{C}$ ,  $0\text{ }^{\circ}\text{C}$ , and  $20\text{ }^{\circ}\text{C}$ . Then, the solution was incubated in the thermal processing tank and taken out using the granite quench. Table 1 details the granite size and the temperature division of the calcium chloride solutions.

**Table 1.** Test material parameters.

| Test Material | Sample Size (L × H × T)<br>(mm) | Hole Size ( $\Phi$ × H)<br>(mm) | Temperature Gradient<br>( $^{\circ}\text{C}$ ) |
|---------------|---------------------------------|---------------------------------|--|
| Granite       | 100 × 100 × 100                 | 30 × 80                         | 150, 350, 550, 750                             |
| Refrigerant   | -                               | -                               | 20, 0, $-30$                                   |

## 2.3. Test Equipment

The granite sample was heated using a BLMT-1200C high-temperature, energy-saving box furnace (Bolemante Experimental Electric Furnace Co., Ltd., Luoyang, China) The maximum temperature of the high-temperature heating furnace could reach  $1200\text{ }^{\circ}\text{C}$ , and the error precision was controlled within  $\pm 2\text{ }^{\circ}\text{C}$ . The heating time and constant temperature could be set to maintain the treatment. The DW-40 type low temperature test chamber was produced by the Xinxing Testing Instrument Company (Cangzhou, China). The test chamber was used for low temperature treatment of calcium chloride solution. The temperature range was between  $-40\text{ }^{\circ}\text{C}$  and  $40\text{ }^{\circ}\text{C}$ , and the actual control temperature error was  $\pm 2\text{ }^{\circ}\text{C}$ . During the test of granite quenching, the dynamic temperature was tracked and recorded by the AS900B noncontact infrared thermometer produced by Xima Instruments (Hong Kong, China). The test temperature range was  $-50\text{ }^{\circ}\text{C}$  to  $900\text{ }^{\circ}\text{C}$ , and the measurement accuracy was  $\pm 2\%$  for continuous recording. The super-eyes B011 digital microscope was produced by the Super-eye Technology Company (Shenzhen, China). The digital microscope was used to observe the crack direction and cracking of the granite surface, and real-time observation was carried out. The maximum magnification was 1000 times, and an object of 0.001 mm could be identified. The detailed experimental equipment is shown in Figure 2a–d.

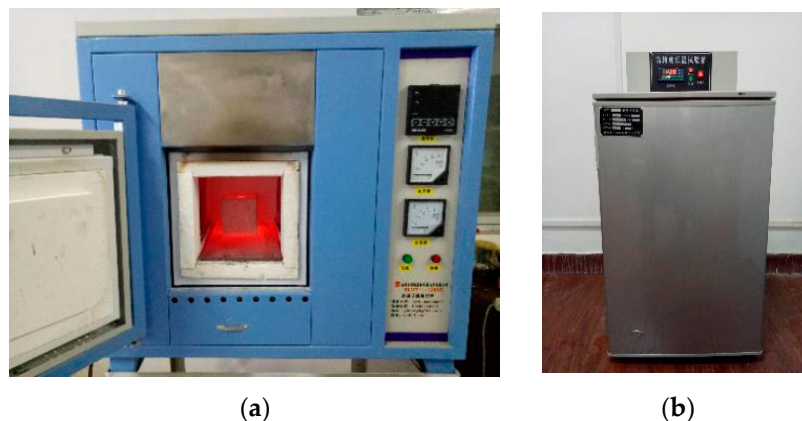


**Figure 2.** Cont.

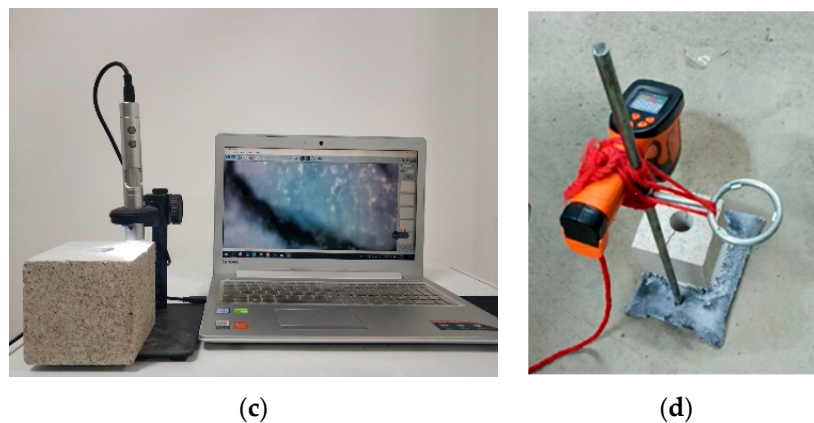


**Figure 2.** Instruments used in the experiment: (a) high temperature box furnace, (b) low temperature box, (c) digital microscope, and (d) infrared radiation thermometers.

### 3. Test Process

Comparative tests of granite at different temperatures under different temperatures of calcium chloride solution were used for this experiment. The granite was heated from room temperature (20 °C) to a preset temperature value using a high-temperature heating furnace. The granite rock samples heated in this test were divided into four temperature gradients—150 °C, 350 °C, 550 °C, and 750 °C—and then the premade calcium chloride solution at different temperatures (−30 °C, 0 °C, and 20 °C) was separately subjected to cooling shock using a low temperature test chamber, and the dynamic processes of the change in temperature in the granite were recorded using an infrared thermometer during the process. After the temperature was lowered to room temperature, the cracking of the rock was observed with a microscope. The detailed experimental process was as follows.

First, the calcium chloride solution had a different freezing point due to the difference in the ratio of calcium chloride to water. In this test, a calcium chloride solution was configured in a ratio of 3:1 of water to anhydrous calcium chloride particles. The solution, with a freezing point that could reach −40 °C, was kept at −30 °C to maintain good fluidity without freezing, and a DW-40 type of low temperature test chamber was used to cool the configured calcium chloride solution to −30 °C. After reaching the preset temperature, the temperature was maintained for 2 hours such that the entire solution could reach −30 °C and was then placed in an incubator. The 0 °C and 20 °C temperatures could be adjusted to the appropriate proportions, and after reaching the preset temperature, were also placed in the incubator to keep warm.

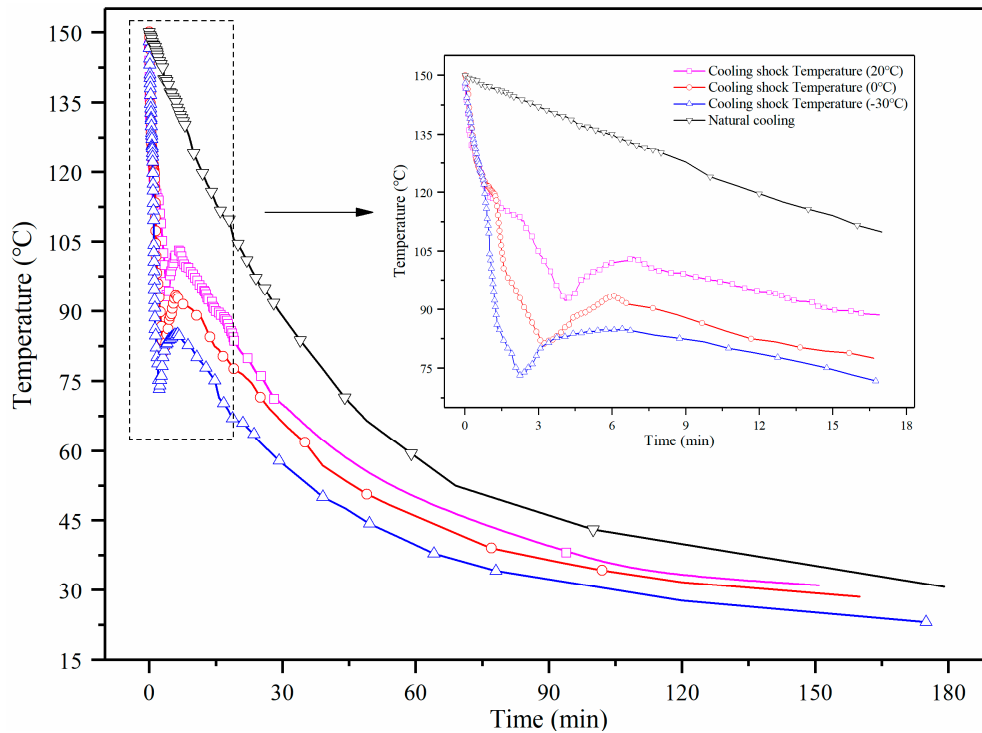
Then, the prefabricated square granite samples were placed in a muffle furnace for the heating treatment, taking into account the influence of the heating rate on the internal structure of the rock [30], preventing the heating rate from being too rapid, which can cause cracking in the interior of the rock, especially with the addition of the muffle furnace. The temperature rate was set to 5 °C/min, and a temperature value was preset in one test, with a total of four temperature gradient values, 150 °C, 350 °C, 550 °C, and 750 °C, the temperature value was set four times for each repeated test. After reaching the preset value, the temperature was kept constant for 2 hours such that the inside of the rock was evenly heated.

Finally, the granite samples heated to a high temperature was quickly removed and a −30 °C calcium chloride solution was injected into the hole until it was full. It should be emphasized that this test only considered the effect of a one-time injection of low-temperature refrigerant solution on the temperature change and crack expansion of granite samples. For this process, the AS900B infrared thermometer was used to record the temperature change at the center of the borehole, and temperature tracking of the granite borehole center was performed. After the sample temperature was lowered to room temperature, the cracking of the outer surface of the granite was observed using a supereyes-B011 microscope.

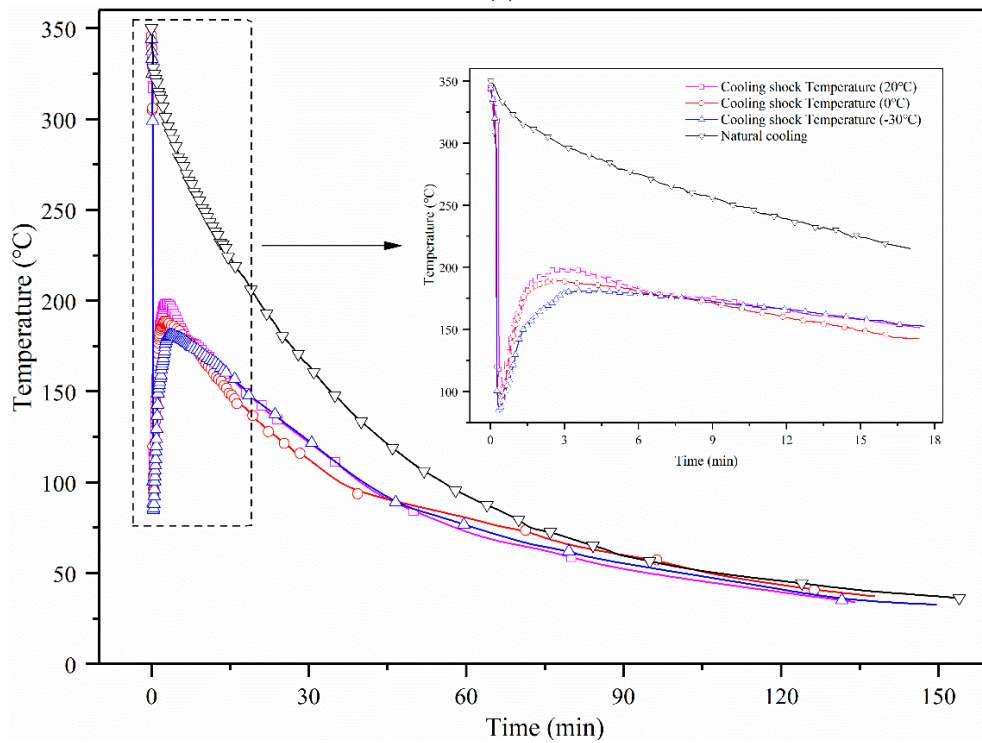
#### 4. Test Results and Analysis

##### 4.1. Comparisons of Temperature Change of High Temperature Granite under Different Cooling Shocks

The temperature evolution curves of high temperature granites heated to 150 °C, 350 °C, 550 °C, and 750 °C under different cooling shock are shown in Figure 3a–d.



(a)



(b)

Figure 3. Cont.

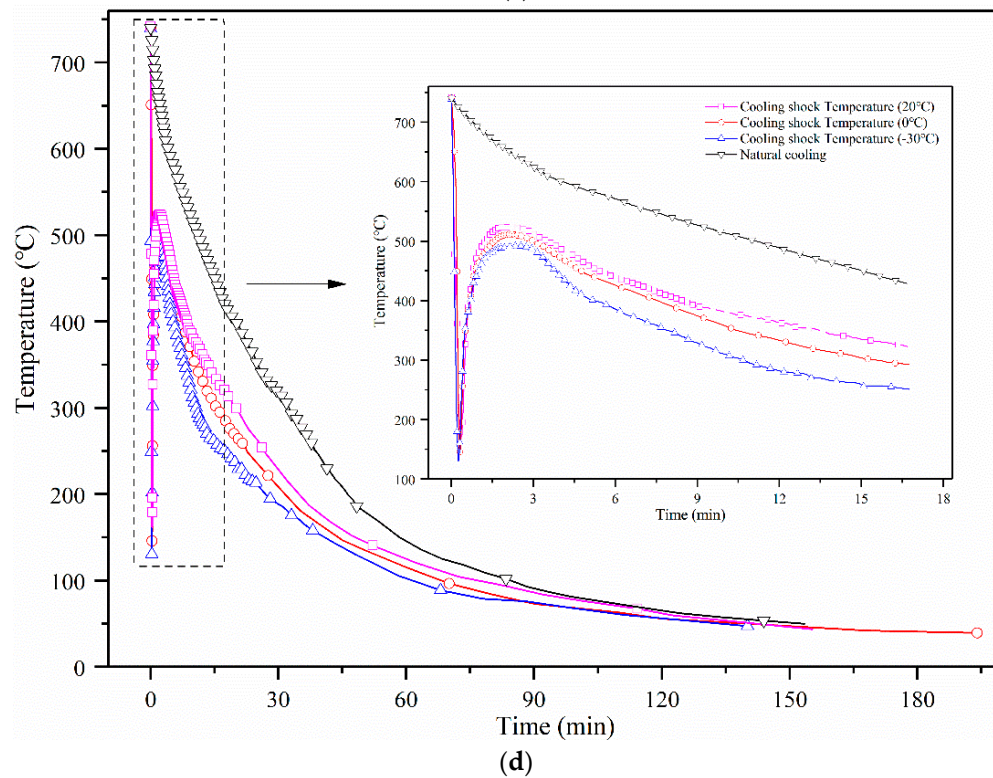
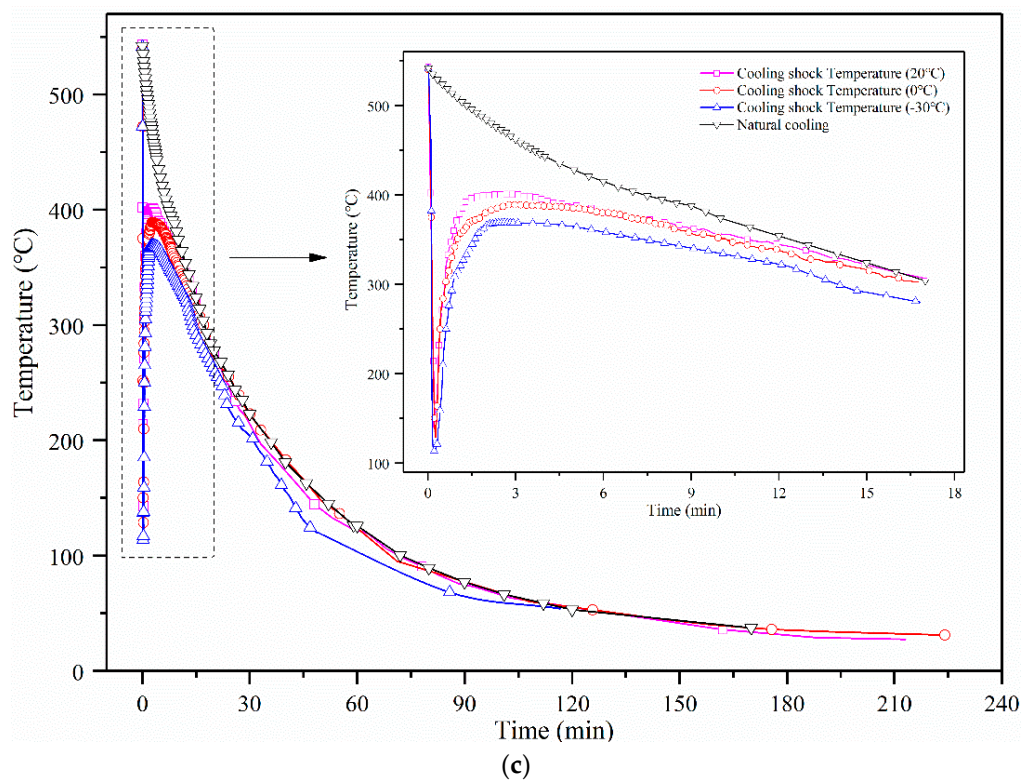


**Figure 3.** Temperature changes of high temperature granite under cooling shock: (a) initial granite temperatures of 150 °C, (b) initial granite temperatures of 350 °C, (c) initial granite temperatures of 550 °C, and (d) initial granite temperatures of 750 °C.

From the temperature curves of the granites with different temperature groups in Figure 3a–d it is understood that due to the injection of calcium chloride solution, a sudden temperature decrease occurred, and as the thermal energy inside the rock mass was gradually transmitted to the low

temperature region of the hole, and the low temperature region of the hole was slowly “heated”. The temperature gradually rose, and when the temperature reached the peak, because the temperature of the air around the granite was much lower than its own temperature, then the granite began to slowly cool until it reached room temperature, as seen from the temperature curve of the granite under the natural cooling condition as the control group, which was slowly cooled down to room temperature.

From the partial enlarged figure, it is seen that due to a cooling shock of  $-30\text{ }^{\circ}\text{C}$ , at the first and lowest point, the point was the lowest point in the entire cooling shock group, followed by the cooling shocks of  $0\text{ }^{\circ}\text{C}$  and  $20\text{ }^{\circ}\text{C}$  to the lowest point of the respective curves. These temperatures then rose back to the peak temperature in about five minutes, then gradually slowed down, and after that, the trend of the cooling shock curve and the cooling curve of the natural cooling control group were gradually more consistent. Therefore, it can be seen from the cooling curve that the granite cracking and energy release mainly occurred during the first five minutes under cold impact, and after that, the trend was not large compared with the temperature change curve under natural cooling, because in the first five minutes, the impact caused by the large temperature difference forced the granite to crack. In the absence of other conditions, the energy released by the subsequent slow cooling was much lower than the energy released by the cooling shock. Thus, the slow cooling after five minutes, had little effect on the cracking of the rock. Table 2 records the measured values of the temperature variation of granite under different cold impacts (without natural cooling) with time. From the values in the table, the specific situations of temperature change can be seen. The impact of the cooling shock at  $-30\text{ }^{\circ}\text{C}$  was the largest, corresponding with the lowest cooling value, as well as the cooling rate also being the largest, and the recovery time required was also longer.

**Table 2.** Statistical results of the temperature change of samples under different cooling shocks.

| Granite Temperature ( $^{\circ}\text{C}$ ) | Refrigerant Temperature ( $^{\circ}\text{C}$ ) | Initial Temperature ( $^{\circ}\text{C}$ ) | Minimum Temperature ( $^{\circ}\text{C}$ ) | Cooling Ratio (%) | Maximum Temperature ( $^{\circ}\text{C}$ ) | Heating Ratio (%) |
|--|--|--|--|-------------------|--|-------------------|
| 150  | 20   | 148  | 92.3                                       | 37.6 ↓            | 103.5                                      | 12.1 ↑            |
|  | 0  | 148  | 81.2                                       | 45.1 ↓            | 93.5                                       | 15.1 ↑            |
|  | $-30$  | 148  | 73.3                                       | 50.5 ↓            | 85   | 16.0 ↑            |
| 350  | 20   | 345  | 101.4                                      | 70.6 ↓            | 198.8                                      | 96.1 ↑            |
|  | 0  | 346  | 93.1                                       | 73.1 ↓            | 188.9                                      | 102.9 ↑           |
|  | $-30$  | 344  | 83.5                                       | 75.7 ↓            | 181  | 116.8 ↑           |
| 550  | 20   | 543  | 142.3                                      | 73.8 ↓            | 401  | 181.8 ↑           |
|  | 0  | 540  | 128.7                                      | 76.2 ↓            | 389  | 202.3 ↑           |
|  | $-30$  | 541  | 113.4                                      | 79.0 ↓            | 369  | 225.4 ↑           |
| 750  | 20   | 742  | 162  | 78.2 ↓            | 524  | 223.5 ↑           |
|  | 0  | 741  | 142.2                                      | 80.8 ↓            | 511  | 259.4 ↑           |
|  | $-30$  | 740  | 130.4                                      | 82.4 ↓            | 492  | 277.3 ↑           |

To show the difference between the cooling segment and the heating segment caused by the cooling shock, a temperature rate analysis for each rock temperature group was carried out, as shown in Figure 4.

The average rate of temperature decrease between the initial temperature of the granite and the lowest temperature after contact with the refrigerant is shown in Figure 4a. The average heating rate of the lowest value of granite rising back to the highest point is shown in Figure 4b. This provides the overall temperature change of the two phases. In the same rock temperature group, the greater the cooling shock is, the higher the cooling rate is, and the smaller the heating rate is. The cooling shock under the same conditions and the corresponding rate increased with the increase in rock temperature, regardless of temperature drop and temperature rise. It can be seen from Figure 5 that the temperature-dependent curves of different high-temperature granite under natural conditions can be approximately divided into three stages. In the first stage of rapid cooling, the thermal interaction

between granite and the surrounding environment was faster in the first 50 min. The higher the granite temperature was, the faster the cooling rate was. The temperature field of the outside air caused a slow cold impact on the granite. However, due to the influence of thermal conductivity and the thermal convection coefficient between the materials [31–33], the cooling effect was smaller than that caused by the calcium chloride solution fluid. The second stage was the slow cooling stage. During this stage, the temperature change curve of granite at different temperatures became a near-linear cooling trend. The third stage was the steady cooling stage. At this stage, the internal temperature of the granite had basically been released, and its own temperature was basically consistent with the external temperature field, tending to a stable state.

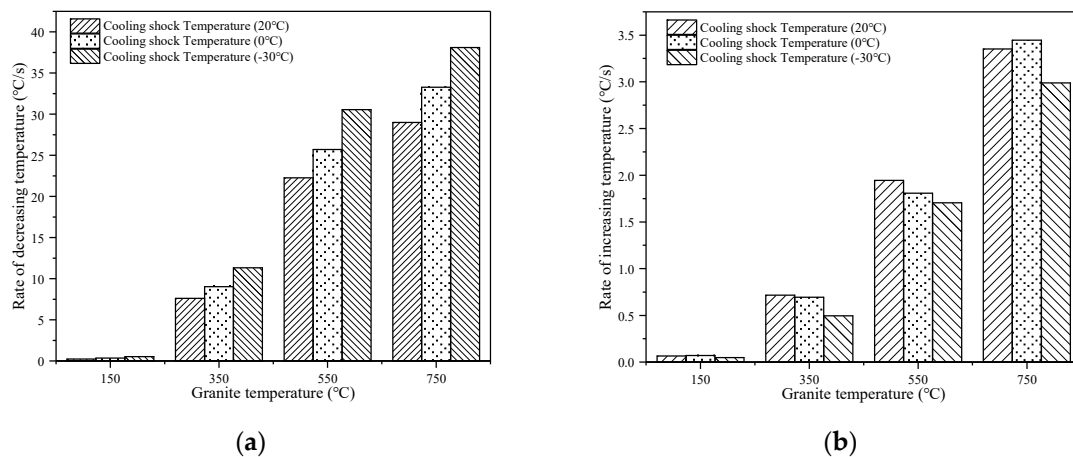


**Figure 4.** The cooling and heating rates for different targeted temperature granite samples: (a) cooling rate and (b) heating rate.

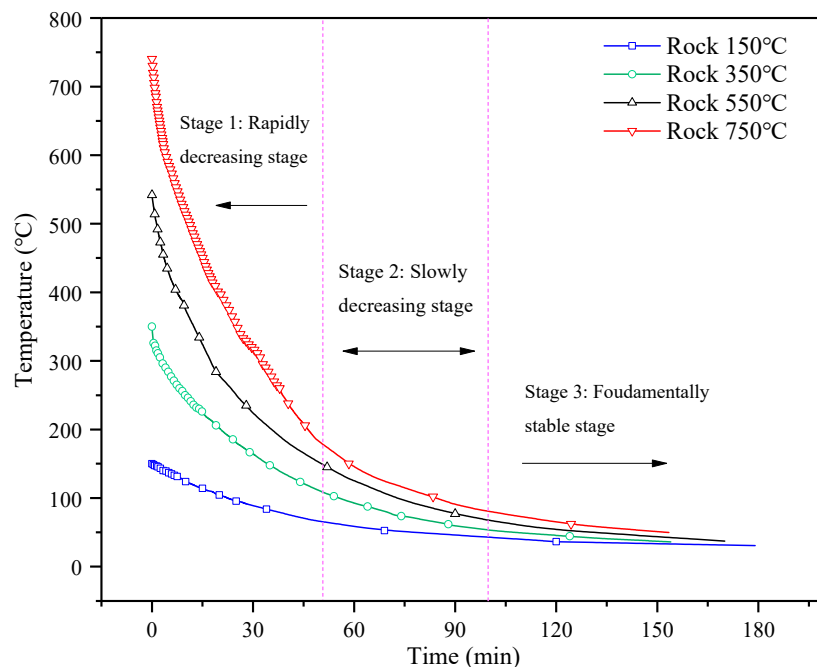


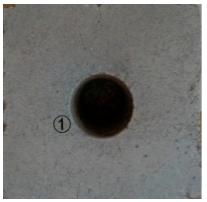
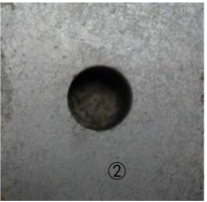
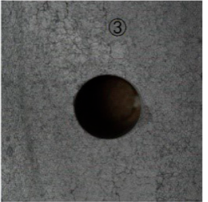
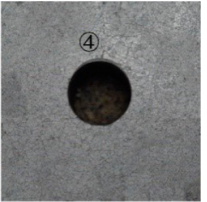
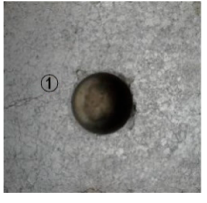
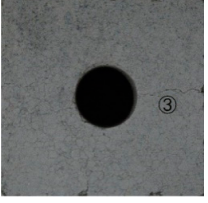
**Figure 5.** Temperature changes of high temperature granite samples under the natural cooling.

#### 4.2. Crack Expansion of High Temperature Granite under Different Cooling Shocks

To observe the surface cracking of rock samples more intuitively, we studied the effect of temperature on the cracking of granite. Therefore, we uniformly sprayed a thin layer of white paint on the surface of the rock samples, which made the cracking of rock samples easier to observe, causing

the cracks to appear more obvious under macroscopic observation. From Tables 3 and 4, we can see the cracking of the granite surface under different cold impacts.

**Table 3.** Comparisons of samples surface cracking features under different cooling shocks.

| Temperature      | Natural Cooling   | Refrigerant (20 °C)   | Refrigerant (0 °C)   | Refrigerant (−30 °C)  |
|------------------|---|---|--|---|
| Granite (150 °C) |    |    |    |    |
| Granite (350 °C) |    |    |    |    |
| Granite (550 °C) |   |   |   |   |
| Granite (750 °C) |  |  |  |  |

**Table 4.** Description of Cracking of Granite.

| Granite Temperature | Refrigerant Temperature | Cracking Condition                                       |
|---------------------|-------------------------|--|
| 150 °C              | 20 °C                   | No crack   |
|                     | 0 °C                    | No crack   |
|                     | −30 °C                  | No crack   |
| 350 °C              | 20 °C                   | No crack   |
|                     | 0 °C                    | A few small cracks                                       |
|                     | −30 °C                  | A few small cracks                                       |
| 550 °C              | 20 °C                   | Small cracks   |
|                     | 0 °C                    | Small cracks and a large through-going fracture          |
|                     | −30 °C                  | Many large through-going fractures                       |
| 750 °C              | 20 °C                   | Many small cracks  |
|                     | 0 °C                    | Many small cracks and a large through-going fracture     |
|                     | −30 °C                  | Many small cracks and many large through-going fractures |

#### 4.2.1. Comparison of Cracking under Different Cooling Shocks at the Same Rock Temperature

It can be seen from Table 3 that under the cold impact of different temperatures in the 150 °C-granite group, there was no obvious cracking, and there were no major changes in the appearance of the

original rock sample. There was a small change in the 350 °C-granite group. It can be seen that microcracks appeared on the surface of the rock sample after cold impact without careful observation using microscopic equipment. However, the overall cracking condition was not obvious. There were no microcracks on the surface of the rock sample under the natural cooling conditions of the comparison group. It was obvious that the cracking condition of the crack was obviously intensified in the 550 °C-granite group. The granite also exhibited obvious cracking conditions under the natural cooling condition. When the temperature difference between the rock layer and the injected fluid was sufficiently high, the thermal stress fracturing was more effective [34,35], and therefore, as the temperature of the calcium chloride solution decreased, the temperature of the granite increased, and the impact force was increased, which resulted in more cracking on the surface of the rock sample and more dispersed microcrack development. The microcracks of these branches gradually developed, connected, and penetrated to finally form a grid-like crack distribution. Under the actions of cooling shock at 0 °C and −30 °C, the through-cracks of the granite surface travelled from the hole to the edge. There were obvious crack distributions on the surface of the 750 °C group, the crack grid was densely distributed, there were many long and wide cracks, and the crack width of the slowly cooling granite was small. The number of cracks under cold impact conditions not only was densely distributed but also had a large crack width and many long cracks. It can be clearly seen that the crack of the granite under the action of the −30 °C cooling shock was wider, and the other end of the hole also had a through-crack. This long crack directly penetrated the surface of the whole granite, and this was not the effect of granite rock samples under other conditions, indicating that under drastic cooling shock conditions, the energy produced created a large contraction force inside the granite, and an outward tensile force was generated on the surface of the granite. This phenomenon occurred under the influence of two forces, and the cohesive force between the rock mineral particles was destroyed, or the mineral particles were directly broken such that the through-crack appeared on the surface of the granite in the macroscopic.

#### 4.2.2. Comparisons of Cracking of Different Rock Temperatures under the Same Cooling Shocks

From the natural temperature-reducing conditions in Table 3, the surface cracking of the rock sample was intensified with the increase of rock temperature, indicating that the high-temperature granite also caused rock cracking during the slow cooling process. Observing the cracking condition of granite under other cooling shock conditions, it can be found that the cracking effect on the surface of the rock sample was more significant. Under the same cooling shock condition, as the rock temperature increased, the microcracks on the surface of the rock sample increased and became denser. The microcracks were gradually connected and penetrated to form dense gridded cracks, and there were long and wide main cracks. These main cracks extended through the hole to the edge, which was more pronounced with the decrease of the cooling shock temperature under the same rock temperature conditions. The anisotropy of granite affected the propagation of cracks [36], and we could also observe the extension of the main crack. Generally, the cracks on the outer boundary of granite were wider, the crack gradually narrowed in the direction of the hole, and as the rock temperature increased, the cooling shock temperature decreased, and the width of the crack also increased. Therefore, compared with the condition of the rock surface cracking under natural cooling conditions, the effects of cold impact on granite damage were still obvious.

## 5. Discussion

### 5.1. Analysis of the Effect of Cold Impact on High Temperature Granite

When the granite was heated to a certain temperature, there was an initial temperature field that was kept at a constant temperature for a period of time. If there was no change in external conditions, it would always be in a constant temperature state, that is, in a thermal equilibrium state. When the calcium chloride solution was injected into the granite hole, it caused a cooling shock to the original

temperature field, breaking the original thermal equilibrium state. Due to the different temperatures of the calcium chloride solution, the range of influence on the granite temperature field was also different. As shown in Figure 3a–d, after applying the cooling shock, the 20 °C refrigerant had the least influence on the temperature field of the granite, with a shorter temperature recovery time, and the –30 °C refrigerant had the largest impact range, with a longer temperature recovery time. When the granite encountered rapid cooling, the lower the temperature the cold impact was, and the higher the temperature of the granite was, the greater the temperature difference between the two and the width of the rock cracking, and therefore, the thermal stress generated by the temperature gradient induced more cracks. Ultimately, this process led to the deterioration of the physical and mechanical properties of granite and the enhancement of permeability [37]. Since the main components of granite are quartz, feldspar, and mica, and their linear expansion is different, and the lattice energy is different, mineral particles will undergo different degrees of thermal damage after experiencing high temperature and cold impact. Therefore, the cold shock caused by different temperature gradients also produced different destructive forces. Moreover, the thermal damage was continuously accumulated inside the granite structure, and the micro-cracks were further developed, aggregated, and connected, thereby exhibiting different degrees of cracking, which ultimately led to a decrease in the mechanical properties of the rock. In addition, focusing on these experiments, the effect of the two temperature fields on the temperature field of the granite, except for the temperature field generated by the calcium chloride solution applied to the central hole, affected the granite, and the indoor air temperature also affected the temperature field of the granite. Since heat will spontaneously transfer from higher temperature zones to lower temperature zones, after the cold impact, the heat inside the rock mass gradually transferred to the hole, thus forming a boundary between the cooling shock and the rock mass. This boundary caused a dynamic heat balance area, and as time increased, the heat balance area continued to narrow toward the hole until the temperature affected by the cooling shock was consistent with the temperature inside the rock mass, which then continued to dissipate heat to the air until the temperature was consistent with the surrounding air. The cold impact of the central hole resulted in a rapid cooling of the granite, which mainly transferred heat to the rock cavity through heat conduction [38], while the air on the outer surface of the granite slowly cooled the granite, mainly radiating heat to the outside of the rock by means of thermal radiation, and had a certain range of influence, with both aspects having affected the cracking of the granite together. Thus, we can distinguish three zones, which are: ① an air impact zone, ② a heat balance zone, and ③ a cooling shock impact zone running from the outer edge to the center of the samples.

To better observe and analyze the crack expansion zone caused by cooling shock, we statistically analyzed the width of some typical through-going cracks of the granite at 550 °C and 750 °C (there were no through macrocracks in the 150 °C and 350 °C groups, but mainly microcracks). Figure 6 is a statistical comparison of the crack widths of the vertical projections generated by the cooling shock of two kinds of temperature granites (the crack number is marked in Table 3). It can be seen from the figure that the crack widths at 750 °C were wider than at 550 °C, and it can also be seen that the greater the temperature gradient of the granite and calcium chloride solution, the greater the impact of the cooling shock, and the wider the cracking width. The thermal damage of the internal structure of the rock was accumulated due to the temperature difference, which caused the crack on the rock surface [39–41]. In the 550 °C group, the natural cooling of the granite and the cracks generated by the cooling shock at 20 °C were not through cracks, but the cooling shock at 0 °C and –30 °C caused through-cracks, and crack widths were larger in cracks closer to the hole. As the number of cracks increased, the permeability and effective flow area increased, which in turn increased the heat transfer efficiency of the fluid in the rock formation [42–44]. In the 750 °C group, due to the increase in the temperature gradient, there were many through cracks, and the crack width of granite increased with the cooling shock at 0 °C and –30 °C, and due to the strong cooling shock, the rock mineral particles directly in contact with the refrigerant generated a strong contraction force, resulting in an increase in the crack width at the hole. Since the outer edge of the rock was not constrained, cracking was

more susceptible on the outer edge of the rock due to the contraction force caused by the cold impact. Therefore, the crack was generated from the outer edge of granite and the center hole, and the two ends changed more severely. The crack width was wider, and then propagated from the two ends to the rock inside along the preferential path, mainly along the grain boundary extension, and gradually merged and penetrated [45]. After the cooling shock on the granite, due to the heat transfer process, there was a heat balance area inside the rock. In this zone, the crack development tended to be a relatively stable condition, so there was no large change in the width of the crack.

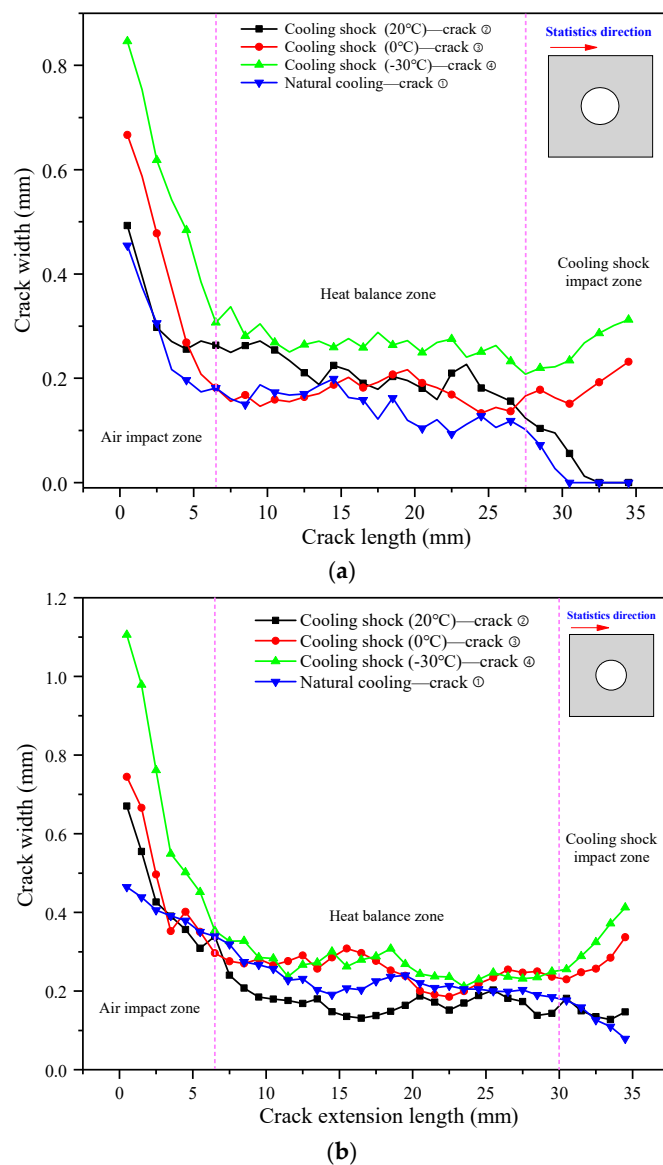


**Figure 6.** Measured results of crack widths along the section direction due to different cooling shocks: (a) measured results of crack widths (550 °C) and (b) measured results of crack widths (750 °C).

### 5.2. Application of Cold Shock Cracking in EGS

Based on the analysis of the impact of the cold shock on granite cracking in this study, the cracking effect was very remarkable. It provided another scheme for the establishment of an enhanced geothermal system. The overall goal of the enhanced geothermal system was to obtain enough heat from underground rock and transport it to the surface for power generation. In order to overcome the problem of insufficient fluidity and permeability of fluids in hot dry rock area, people usually adopt the strategy of reforming a geothermal system using normal temperature hydraulic fracturing to

improve rock porosity and permeability. The test results show that the granite fracturing effect after a cold shock is better. We can consider replacing a normal temperature fracturing fluid with a lower temperature fracturing fluid to achieve a better fracturing effect, which can generate wider and more stable fracture and a denser micro-fracture network, which can greatly improve heat flow, permeability, and porosity, and thus improve extraction efficiency. In addition, the process of heat extraction in a geothermal reservoir is a slow cooling process for the surrounding rock mass. The effect of slow cooling on granite cracking cannot be neglected under natural cooling conditions, the loss of fluid from microcracks should be prevented, thereby increasing the recovery rate of heat extraction. From the statistics of the change of the temperature change curve of this test, the lower the cold shock, the better the cracking effect and the slower the recovery time. Therefore, the curve relationship between the temperature and time of the test and the cracking effect can provide a reference for simulating the variation of the temperature field of the surrounding rock and the threshold of failure over time. In addition, in the extraction of geological resources, with the drilling going deep, the temperature got higher and higher, and the influence of the high temperature on the strength of drill bit was getting stronger and stronger. If the refrigerant is introduced into drilling fluid, it can not only cool the bit, but also cold impact on the drilling rock, making it more fractured, easier to drill, and improves the rock breakage rate.

## 6. Conclusions

In this study, the granite was first heated to different temperatures, and then the calcium chloride solution was cooled to a different temperature. Finally, the calcium chloride solution was injected into the granite hole to cause rapid cooling and a cold impact. In addition, as a control group, the temperature was slowly cooled under natural cooling conditions. The temperature of the granite was tracked during this cooling process, and a statistical analysis of the damage caused by the two cooling modes was conducted. According to these test results and subsequent data analysis, the following conclusions were obtained:

- (1) In the experiment regarding comparative analysis of the temperature-dependent evolution law of high-temperature granite under different cold impacts, it was seen that the dramatic changes cooling effect caused by the strong cooling shock on the high temperature granite usually occurred within the first 5 min of the rapid cooling phase, and when the temperature of the rock increased, the change was more significant and the occurrence time was shorter. Different cooling shocks occurred for approximately 120 min, and the trend of temperature changes and the trend of slow cooling were similar. From the temperature curves of the four groups of granites heated to different temperatures, the cold impact effects of the 550 °C and 750 °C granites were visibly greater than those of the 150 °C and 350 °C groups. Therefore, the temperature threshold for the cooling shock to have a significant cooling effect should be between 350 °C and 550 °C.
- (2) By studying the cracking conditions of high-temperature granite under a cooling shock, it can be seen that the effect of rapid cooling under cold impact on the cracking effect of high-temperature granite was much greater than that caused by slow cooling. In this study, granites with temperatures of 550 °C and 750 °C showed large through-cracks under the action of cooling shock at −30 °C, which indicated that the greater the temperature gradient generated, the more intense the damage was to the rock mass. The increase of cold impact resulted in internal shrinkage of the rock mass, external stretching, wider cracks, and denser mesh formed by microcracks. In the area affected by cooling shock, the closer the crack was to the cold impact source, the wider the crack width is, and the crack width gradually narrowed further away from the cold source. In the dynamic heat balance region, there was no large temperature gradient, and the development of cracks was generally relatively stable.
- (3) This study provides a new method of using cooling shock to crack rock masses in the establishment of dry heat rock reservoir area. It can be observed that crack expansion after cooling shock was much better. Therefore, to achieve significant cracks, we can consider replacing normal

temperature fluid with a lower temperature fluid. In addition, cooling shock would cause wider cracks and denser microcracks, with the refrigerant liquid continuously flowing into these microcracks, such that these microcracks are further enlarged, the effect of cracking will be greatly improved, and the permeability will be increased, thereby extracting more heat. In addition, it can be seen from the test that microcracks caused by the slow cooling of rock were not as serious as those caused by rapid cooling; however, in the design and exploitation of deep thermal reservoirs, such as for geothermal energy, the effects of slow cooling on the rock mass near the thermal reservoir cannot be ignored.

**Author Contributions:** Y.-J.S. and X.H. conceived and designed the experiments; X.H. and J.-Q.Y. performed the experiments and analyzed the data; Y.-J.S. and C.-H.Z. contributed funding supports; X.H. wrote the paper. Y.-J.S. revised the English of this paper.

**Funding:** This research was funded by the National Natural Science Foundation of China (Grant No. 41772333); the Natural Science Foundation of Shaanxi Province, China (Grant No. 2018JQ5124); and the Foundation from State Key Laboratory for Geo-Mechanics and Deep Underground Engineering, China University of Mining & Technology (Grant No. SKLGDUEK1813).

**Acknowledgments:** We thank the entire team for their efforts and the reviewers for their valuable comments to improve the quality of the article. At the same time, we would like to thank editor for his timely handling of the manuscripts.

**Conflicts of Interest:** The authors declare no conflicts of interest.

## References

1. Rohde, R.; Muller, R.A.; Jacobsen, R.; Muller, E.; Wickham, C. A new estimate of the average earth surface land temperature spanning 1753 to 2011. *Geoinfor. Geostat. Overv.* **2013**, *1*. [[CrossRef](#)]
2. Solomon, S.; Qin, D.; Manning, M.; Chen, Z.; Margiquis, M.; Averyt, K.B.; Tignor, M.; Miller, H.L. *Climate Change 2007: The Physical Science Basis, Contribution of Working Group to the Fourth Assessment Report of the Intergovernmental Panel on Climate Change (IPCC)*; Cambridge University Press: Cambridge, UK, 2007; pp. 434–497.
3. Clauser, C.; Ewert, M. The renewables cost challenge: Levelized cost of geothermal electric energy compared to other sources of primary energy—Review and case study. *Renew. Sustain. Energy Rev.* **2018**, *82*, 3683–3693. [[CrossRef](#)]
4. Speight, J. Geothermal energy: Renewable energy and the environment, second edition, by William E. Glassley. *Energy Sources* **2015**, *37*, 2039. [[CrossRef](#)]
5. Shen, Y.J.; Wang, Y.Z.; Yang, Y.; Sun, Q.; Luo, T.; Zhang, H. Influence of surface roughness and hydrophilicity on bonding strength of concrete-rock interface. *Constr. Build. Mater.* **2019**, *213*, 156–166. [[CrossRef](#)]
6. Oganov, A.R. Thermodynamics, phase transitions, equations of state, and elasticity of minerals at high pressures and temperatures. *Treatise Geophys.* **2015**, *2*, 179–202. [[CrossRef](#)]
7. Yang, S.Q.; Ranjith, P.G.; Jing, H.-W.; Tian, W.-L.; Ju, Y. An experimental investigation on thermal damage and failure mechanical behavior of granite after exposure to different high temperature treatments. *Geothermics* **2017**, *65*, 180–197. [[CrossRef](#)]
8. Yin, T.B.; Shu, R.H.; Li, X.B.; Wang, P.; Liu, X.L. Comparison of mechanical properties in high temperature and thermal treatment granite. *Trans. Nonferrous Metals Soc. China* **2016**, *26*, 1926–1937. [[CrossRef](#)]
9. Guo, L.-L.; Zhang, Y.-B.; Zhang, Y.-J.; Yu, Z.-W.; Zhang, J.-N. Experimental investigation of granite properties under different temperatures and pressures and numerical analysis of damage effect in enhanced geothermal system. *Renew. Energy* **2018**, *126*, 107–125. [[CrossRef](#)]
10. Araújo, R.G.S.; Sousa, J.L.A.O.; Bloch, M. Experimental investigation on the influence of temperature on the mechanical properties of reservoir rocks. *Int. J. Rock Mech. Min.* **1997**, *34*, 2980.e1–2980.e16. [[CrossRef](#)]
11. Huang, Y.H.; Yang, S.Q.; Hall, M.R.; Tian, W.L.; Yin, P.F. Experimental study on uniaxial mechanical properties and crack propagation in sandstone containing a single oval cavity. *Arch. Civ. Mech. Eng.* **2018**, *18*, 1359–1373. [[CrossRef](#)]
12. Zhang, P.; Mishra, B.; Heasley, K.A. Experimental investigation on the influence of high pressure and high temperature on the mechanical properties of deep reservoir rocks. *Rock Mech. Rock Eng.* **2015**, *48*, 2197–2211. [[CrossRef](#)]

13. Freire-Lista, D.M.; Fort, R.; Varas-Muriel, M.J. Thermal stress-induced microcracking in building granite. *Eng. Geol.* **2016**, *206*, 83–93. [[CrossRef](#)]
14. Wang, H.F.; Bonner, B.P.; Carlson, S.R.; Kowallis, B.J.; Heard, H.C. Thermal stress cracking in granite. *J. Geophys. Res.* **1989**, *94*, 1745. [[CrossRef](#)]
15. Zhao, Z. Thermal influence on mechanical properties of granite: A microcracking perspective. *Rock Mech. Rock Eng.* **2015**, *49*, 747–762. [[CrossRef](#)]
16. Hosseini, M. Effect of temperature as well as heating and cooling cycles on rock properties. *J. Min. Environ.* **2017**, *8*, 631–644. [[CrossRef](#)]
17. Thirumalai, K.; Demou, S.G. Thermal expansion behavior of intact and thermally fractured mine rocks. *Evolution* **1974**, *53*, 147–156. [[CrossRef](#)]
18. Griffiths, L.; Lengliné, O.; Heap, M.J.; Baud, P.; Schmittbuhl, J. Thermal cracking in westerly granite monitored using direct wave velocity, coda wave interferometry, and acoustic emissions. *J. Geophys. Res. Solid Earth* **2018**. [[CrossRef](#)]
19. Todd, T.P. *Effect of Cracks on Elastic Properties of Low Porosity Rocks*; Massachusetts Institute of Technology: Cambridge, MA, USA, 1973.
20. Isaka, B.; Gamage, R.; Rathnaweera, T.; Perera, M.; Chandrasekharam, D.; Kumari, W. An influence of thermally-induced micro-cracking under cooling treatments: Mechanical characteristics of Australian granite. *Energies* **2018**, *11*, 1338. [[CrossRef](#)]
21. Kim, K.; Kemeny, J.; Nickerson, M. Effect of rapid thermal cooling on mechanical rock properties. *Rock Mech. Rock Eng.* **2013**, *47*, 2005–2019. [[CrossRef](#)]
22. Kumari, W.G.P.; Ranjith, P.G.; Perera, M.S.A.; Chen, B.K.; Abdulagatov, I.M. Temperature-dependent mechanical behaviour of Australian Strathbogie granite with different cooling treatments. *Eng. Geol.* **2017**, *229*, 31–44. [[CrossRef](#)]
23. Shao, S.; Wasantha, P.L.P.; Ranjith, P.G.; Chen, B.K. Effect of cooling rate on the mechanical behavior of heated Strathbogie granite with different grain sizes. *Int. J. Rock Mech. Min.* **2014**, *70*, 381–387. [[CrossRef](#)]
24. Kumari, W.G.P.; Ranjith, P.G.; Perera, M.S.A.; Chen, B.K. Experimental investigation of quenching effect on mechanical, microstructural and flow characteristics of reservoir rocks: Thermal stimulation method for geothermal energy extraction. *J. Petrol. Sci. Eng.* **2018**, *162*, 419–433. [[CrossRef](#)]
25. Siratovich, P.A.; Villeneuve, M.C.; Cole, J.W.; Kennedy, B.M.; Bégué, F. Saturated heating and quenching of three crustal rocks and implications for thermal stimulation of permeability in geothermal reservoirs. *Int. J. Rock Mech. Min.* **2015**, *80*, 265–280. [[CrossRef](#)]
26. Cai, C.; Li, G.; Huang, Z.; Tian, S.; Shen, Z.; Fu, X. Experiment of coal damage due to super-cooling with liquid nitrogen. *J. Nat. Gas Sci. Eng.* **2015**, *22*, 42–48. [[CrossRef](#)]
27. Li, R.; Huang, Z.; Wu, X.; Yan, P.; Dai, X. Cryogenic quenching of rock using liquid nitrogen as a coolant: Investigation of surface effects. *Int. J. Heat Mass Transf.* **2018**, *119*, 446–459. [[CrossRef](#)]
28. Wu, X.G.; Huang, Z.W.; Li, R.; Zhang, S.K.; Wen, H.T.; Huang, P.P.; Dai, X.; Zhang, C. Investigation on the damage of high-temperature shale subjected to liquid nitrogen cooling. *J. Nat. Gas Sci. Eng.* **2018**, *57*, 284–294. [[CrossRef](#)]
29. Hou, J.; Cao, M.; Liu, P. Development and utilization of geothermal energy in China: Current practices and future strategies. *Renew. Energy* **2018**, *125*, 401–412. [[CrossRef](#)]
30. Zuo, J.P.; Xie, H.P.; Zhou, H.W.; Peng, S.P. Experimental research on thermal cracking of sandstone under different temperature. *Chin. J. Geophys.* **2007**, *50*, 1150–1155. [[CrossRef](#)]
31. Abdallah, G.; Thoraval, A.; Sfeir, A.; Pigué, J.P. Thermal convection of fluid in fractured media. *Int. J. Rock Mech. Min.* **1995**, *32*, 481–490. [[CrossRef](#)]
32. Tang, S.B.; Zhang, H.; Tang, C.A.; Liu, H.Y. Numerical model for the cracking behavior of heterogeneous brittle solids subjected to thermal shock. *Int. J. Solids Struct.* **2016**, *80*, 520–531. [[CrossRef](#)]
33. Vosteen, H.D.; Schellschmidt, R. Influence of temperature on thermal conductivity, thermal capacity and thermal diffusivity for different types of rock. *Phys. Chem. Earth Parts A/B/C* **2003**, *28*, 499–509. [[CrossRef](#)]
34. Kitao, K.; Arikawa, K.; Hatakeyama, K.; Wakita, K. Well stimulation using cold-water injection experiments in the Sumikawa geothermal field, Akita prefecture, Japan Transactions. In Proceedings of the Geothermal Resources Council 1990 Annual Meeting, Kailua-Kona, HI, USA, 20–24 August 1990; Volume 14, pp. 1219–1224.
35. Olsson, R.; Barton, N. An improved model for hydromechanical coupling during shearing of rock joints. *Int. J. Rock Mech. Min.* **2001**, *38*, 317–329. [[CrossRef](#)]

36. Freire-Lista, D.M.; Fort, R. Exfoliation microcracks in building granite. Implications for anisotropy. *Eng. Geol.* **2017**, *220*, 85–93. [[CrossRef](#)]
37. Chaki, S.; Takarli, M.; Agbodjan, W.P. Influence of thermal damage on physical properties of a granite rock: Porosity, permeability and ultrasonic wave evolutions. *Constr. Build. Mater.* **2008**, *22*, 1456–1461. [[CrossRef](#)]
38. Zhang, B.T.; Ling, G.F.; Wu, J.Q. New thinking, method and calculated examples of high temperature thermochronology of granite plutons. *J. Geo. Chin. Univ.* **2013**, *19*, 385–402. [[CrossRef](#)]
39. Zhao, Y.; Feng, Z.; Xi, B.; Wan, Z.; Yang, D.; Liang, W. Deformation and instability failure of borehole at high temperature and high pressure in hot dry rock exploitation. *Renew. Energy* **2015**, *77*, 159–165. [[CrossRef](#)]
40. Shen, Y.J.; Zhang, Y.L.; Gao, F.; Yang, G.S.; Lai, X.P. Influence of temperature on the microstructure deterioration of sandstone. *Energies* **2018**, *11*, 1753. [[CrossRef](#)]
41. Shen, Y.J.; Yang, Y.; Yang, G.S.; Hou, X.; Ye, W.J.; You, Z.M.; Xi, J.M. Damage characteristics and thermo-physical properties changes of limestone and sandstone during thermal treatment from  $-30\text{ }^{\circ}\text{C}$  to  $1000\text{ }^{\circ}\text{C}$ . *Heat Mass Transf.* **2018**, *54*, 3389–3407. [[CrossRef](#)]
42. Zhao, Z. On the heat transfer coefficient between rock fracture walls and flowing fluid. *Comput. Geotech.* **2014**, *59*, 105–111. [[CrossRef](#)]
43. Al-Rbeawi, S. How much stimulated reservoir volume and induced matrix permeability could enhance unconventional reservoir performance. *J. Nat. Gas. Sci. Eng.* **2017**, *46*, 764–781. [[CrossRef](#)]
44. O’Sullivan, M.J.; Pruess, K.; Lippmann, M.J. State of the art of geothermal reservoir simulation. *Geothermics* **2001**, *30*, 395–429. [[CrossRef](#)]
45. Kumari, W.G.P.; Ranjith, P.G.; Perera, M.S.A.; Li, X.; Li, L.H.; Chen, B.K.; Avanthi Isaka, B.L.; de Silva, V.R.S. Hydraulic fracturing under high temperature and pressure conditions with micro CT applications: Geothermal energy from hot dry rocks. *Fuel* **2018**, *230*, 138–154. [[CrossRef](#)]



© 2019 by the authors. Licensee MDPI, Basel, Switzerland. This article is an open access article distributed under the terms and conditions of the Creative Commons Attribution (CC BY) license (<http://creativecommons.org/licenses/by/4.0/>).